Emulsion Polymerization in a Hybrid Carbon Dioxide/Aqueous Medium

Murat A. Quadir,[†] Rodd Snook,[‡] Robert G. Gilbert,*[,‡] and Joseph M. DeSimone*[,†]

Department of Chemistry, University of North Carolina at Chapel Hill CB# 3290, Venable and Kenan Laboratories, Chapel Hill, North Carolina 27599-3290, and School of Chemistry, University of Sydney, NSW 2006, Australia

Received February 25, 1997; Revised Manuscript Received July 11, 1997[⊗]

ABSTRACT: The development of a new reaction medium is reported, based on a biphasic mixture of carbon dioxide and water for emulsion polymerizations: a surfactant-free aqueous emulsion polymerization of methyl methacrylate using potassium persulfate under a varying head pressure of CO_2 (0−350 bar) at 75 °C. The resulting polymer is a stable latex with particles of submicron size. The effect of CO_2 on polymerization is relatively small, until there is a significant change at high CO_2 pressure. This is seen by examining the molecular weight distribution in the form of the log(number distribution), $P(M)$ (readily obtained by GPC). At pressures of 140 bar and below, the $P(M)$ show the form expected for chain-stopping events dominated by transfer and by diffusion-controlled termination. At 280 bar, ln $P(M)$ is significantly steeper than its lower-pressure counterpart at relatively low conversion (45%). This is attributed to swelling by supercritical CO_2 reducing the viscosity of the particles, allowing more rapid termination.

Introduction

Carbon dioxide has recently been employed as an inert medium for a variety of free-radical reactions.[1] For example, we have recently reported dispersion polymerizations in a carbon dioxide continuous phase resulting in spherical colloidal particles of poly(methyl methacrylate) using CO_2-soluble amphiphiles.[1,2] Previous reports have also detailed solution[3] and precipitation[4] polymerizations in carbon dioxide.

Because carbon dioxide and water exhibit low mutual solubilities, the combination of carbon-dioxide-based processes and conventional aqueous heterogeneous polymerization processes is similar to the biphasic fluorocarbon/hydrocarbon system for olefin hydroformylation recently reported by Horvath[5] and provides a substantial departure from current technologies, allowing for the compartmentalization of monomer, polymer, and initiator based on their solubility characteristics. Furthermore, the tunability inherent to supercritical fluids allows one to vary the density, viscosity, and solvent strength of the carbon dioxide phase with simple changes in pressure or temperature. It is well-known that carbon dioxide significantly plasticizes many polymer particles,[6] allowing one to tune not only the solvent environment but potentially the glass transition temperature, melting temperature, and viscosity of the polymer-rich particles being formed. This could produce qualitative changes in kinetics, molecular weight distributions, etc., since, for example, it could lead to different mechanisms for reactions such as termination, which are normally diffusion-controlled.[7] This might lead to qualitatively different molecular weight distributions (MWDs) with changing pressure of CO_2, with a concomitant reduction in the gel effect being manifest in the kinetics. The advantages of using CO_2 here, rather than a more common liquid organic solvent are 3-fold. Firstly, environmental considerations make CO_2 a much more responsible choice than liquid organic solvents. Secondly, solvent removal is achieved simply by careful venting of the system. Lastly, CO_2 has a viscosity that is, under the conditions used, significantly lower than that of conventional liquid solvents and would thus be expected to have a greater impact on reaction kinetics.

These biphasic systems are ideally suited for handling highly reactive monomers such as chloroprene or tetrafluoroethylene, where monomer dilution with inert carbon dioxide can serve to moderate reactivity. Also, water's high heat capacity can be advantageous in controlling exothermic polymerizations. Herein, we report the detailed characterization of a methyl methacrylate emulsion polymerization using such a hybrid system.[8−11]

The reaction mechanism for a traditional surfactant-free emulsion polymerization in an aqueous continuous phase with an initiator such as persulfate is generally referred[7] to as following a "homogeneous-coagulative nucleation" process.[12−14] An initiator molecule in the aqueous phase undergoes aqueous-phase propagation and termination, until it reaches a degree of polymerization z when it can either enter a preexisting particle or grow further to a degree of polymerization j_{crit}. An oligomeric radical of size j_{crit} may homogeneously nucleate to form a new (precursor) particle. Precursor particles are colloidally unstable, and grow by both propagation and by coagulation until they achieve sufficient size and charge density to become stable to further coagulation. Colloidal stability is provided by in situ surfactant, i.e., the end groups arising from initiator dissociation (which are either oligomeric species formed from aqueous-phase termination or grafted long chains). Because the amount of such in situ surfactant is comparatively small, latex particles formed in a "surfactant-free" emulsion polymerization are usually large. Interval 1 denotes the period of particle formation, when newly formed radicals may form new particles. Interval 2 denotes the period of particle growth in the absence of new particle formation (i.e., when the only fates available to newly formed radicals are either aqueous-phase termination or entry into a preexisting particle) in the presence of monomer droplets. Interval 3 denotes the final period of particle

* To whom correspondence should be addressed.
[†] University of North Carolina at Chapel Hill.
[‡] University of Sydney.
[⊗] Abstract published in *Advance ACS Abstracts,* September 1, 1997.

S0024-9297(97)00259-3 CCC: $14.00

growth, when droplets have disappeared and monomer is contained only in the particles and (usually to a much smaller extent) in the continuous phase.

The present system comprises water and high-pressure CO_2. Visual inspection of the system showed that there were always two continuous phases present (in addition to the particle phase), a water-rich and a CO_2-rich phase. These phases remain separate, and under low agitation a clear phase boundary was seen between the upper CO_2-rich phase and the lower water-rich phase. Polymer particles were observed only in the water-rich phase, with no visible creaming (accumulation at an interface).

Experimental Section

Surfactant-free emulsion polymerization of methyl methacrylate was conducted in a 10 mL high-pressure view cell that has been previously described.[15,16] In all cases, the reactor was purged thoroughly with argon prior to use. An aqueous solution (5.0 mL) of potassium persulfate (Aldrich, used as received) and 1.0 mL of methyl methacrylate were charged before the cell was filled with CO_2. The reactor was then heated to 75 °C and kept at constant temperature for various times, typically 4 h. After the allotted reaction time, the cell was cooled and the upper carbon dioxide phase, which occupied approximately half of the reaction vessel, was vented. The white stable latex was collected and freeze-dried. Conversion was then determined gravimetrically.

Particle size distributions were determined using capillary hydrodynamic fractionation (CHDF).[17,18] Each sample was sonicated for 5 min before dilution with eluent (Matec Applied Sciences 2X-GR500) to a polymer weight fraction of approximately 2% for analysis. Duplicate or triplicate injections of each sample were made into a capillary hydrodynamic fractograph (Matec Applied Sciences, model CHDF-1100 with C-570 cartridge). Deconvolution of the resultant particle size distribution (PSD) was performed only if the results were reproducible between injection. Samples showing a significant detector response from residual monomer were dried in air at room temperature for several hours to remove residual monomer, and enhance the accuracy of the PSD obtained. Particles were also examined using scanning electron microscopy.

Molecular weight distributions were obtained from these samples as follows. Polymer latex samples were dried in an air oven at 50 °C overnight. Solutions of the dried polymer (0.4% w/v in THF) were injected into a gel permeation chromatograph (Millipore Waters Associates Liquid Chromatograph). Using THF as a mobile phase, the sample was eluted through 10^6, 10^4, and 10^3 Å size-exclusion columns (Waters Ultrastyragel) in series. Detection of eluted polymer was achieved by refractometry (Millipore Waters Associates differential refractometer, model R401).

Expected Form of Molecular Weight Distributions

A useful way of obtaining qualitative and quantitative information from an experimental MWD is as the *instantaneous number distribution* $P(M)$.[7,19] The *cumulative* number distribution, $\bar{P}(M)$, is related to the GPC trace $G(V_{el})$ by[19,20]

$$\bar{P}(M) = \frac{G(V_{el})}{M} \frac{dV_{cal}}{dM}\Big|_{V_{cal}(M)=V_{el}} \qquad (1)$$

where M is molecular weight, V_{el} is the elution volume, and the function $V_{cal}(M)$ is the GPC calibration curve. In the common case of a linear calibration (i.e., $V_{cal}(M) = a + b \log M$), then one has simply

$$\bar{P}(M) = (\text{normalization const}) \times \frac{G(V_{el})}{M^2} \qquad (2)$$

If transfer to monomer is the dominant chain-stopping event, then one has

$$P(M) \propto \exp\left(-\frac{k_{tr}}{k_p}\frac{M}{M_0}\right) \qquad (3)$$

where M_0 is the molecular weight of a monomer unit, and thus M/M_0 is the degree of polymerization; the proportionality constant omitted in eq 3 is trivially given by the total mass of polymer; k_{tr} and k_p are the rate coefficients for transfer to monomer and propagation, respectively. Similarly, in a system where termination is the dominant chain-stopping event, and where (as is always expected to be the case in heterogeneous polymerizations such as the present where virtually all polymerization occurs at polymer concentrations in excess of where entanglements set in) termination is dominated by diffusive encounters between long and short radicals,[21] one has[19]

$$\lim_{M\to\infty} P(M) \propto \exp\left(-\frac{k_{tr}[M] + \langle k_t\rangle[R]}{k_p[M]}\frac{M}{M_0}\right) \qquad (4)$$

where [M] and [R] are the concentrations of monomer and radicals and $\langle k_t\rangle$ is the average termination rate coefficient, this average being over all chain lengths. Equation 4 is applicable to "pseudo-bulk" emulsion polymerization kinetics,[7] which is the type followed by methyl methacrylate.[7,22]

Equations 3 and 4 suggest that one should plot the instantaneous number MWD as ln $P(M)$ against M, when a linear portion at higher molecular weights is always expected. Formally, one defines[23] the dimensionless quantity Λ by

$$\lim_{M\to\infty}\left(\frac{\ln P(M)}{M}\right) \equiv -\frac{\Lambda}{M_0} \qquad (5)$$

For example, Λ would be the transfer constant to monomer if this were the only chain-stopping event or, more generally, $(k_{tr}[M] + \langle k_t\rangle[R])/k_p[M]$. One can compare experimental and theoretical values of Λ.

Now, experimental MWDs are always obtained as the *cumulative* distribution. While (pseudo-)instantaneous MWDs can be obtained by subtraction of cumulative MWDs obtained at successive conversions (e.g., ref 23), in practice it is often found that the expected high-M linearity is obtained even for cumulative distributions, since much of the high-M polymer is often formed over a conversion range close to that at which the sample is taken (since the rate of chain-stopping invariably decreases with conversion). To show this in detail, some MWDs for the present system were simulated to aid data interpretation, with all parameters either from the literature[7] or as follows. Because MMA follows "pseudo-bulk" kinetics with 100% initiator efficiency in an emulsion polymerization system,[7,23] both the inter- and the intraparticle kinetics controlling the MWDs are particularly simple to model, requiring only the rate coefficients for initiator dissociation, transfer to monomer, and propagation, together with a model for how the diffusion coefficient of oligomeric radicals scales with conversion and with the degree of polymerization, and the diffusion coefficient of monomer as a function of conversion. $[M_W] = 0.025$ mol dm^{-3} was taken to be the same as that in a CO_2-free system at 50 °C, as was the equilibrium monomer concentration inside the particles (both these may, however, be significantly

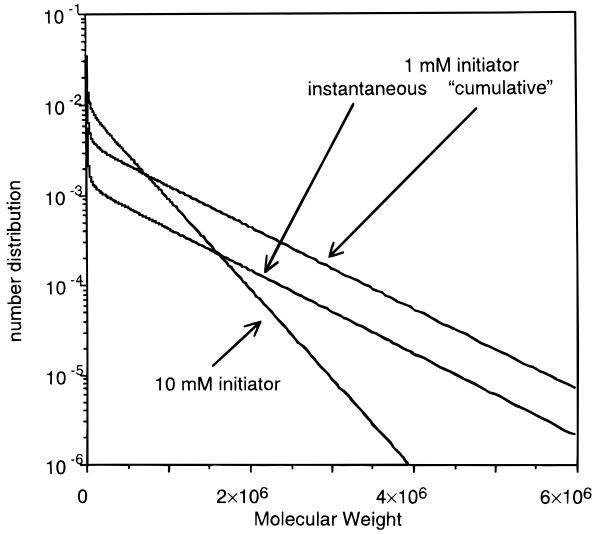

Figure 1. Simulated instantaneous number MWDs (on a $\log_{10}$ scale) at 75 °C, $N_c = 3 \times 10^{15}$ dm^{-3}, using the model of Clay and Gilbert,[19] with all rate parameters as given in the text. Instantaneous distributions for 1 and 10 mM initiator at $w_p = 0.4$ are shown, as is the "cumulative" distribution obtained by summing the contributions from $P(M)$ calculated at $w_p = 0.3$, 0.4, and 0.5.

altered by the presence of CO_2). The rate coefficient for transfer to monomer, k_{tr}, was taken as 6×10^{-2} dm^3 mol^{-1} s^{-1} (from the value at 50 °C [24] and by assuming a 20 kJ mol^{-1} activation energy), $k_p = 1.17 \times 10^3$ dm^3 mol^{-1} s^{-1},[25,26] initiator dissociation rate coefficient $k_d = 4.4 \times 10^{-5}$ s^{-1}, and a water-phase termination rate coefficient of oligomeric radicals $= 4 \times 10^9$ dm^3 mol^{-1} s^{-1}. It has been suggested that the value of the degree of polymerization for entry for MMA might be $z = 5$ at 50 °C,[27] this value being consistent with the observation that initiator efficiency is very high for this monomer in emulsion polymerizations.[7,28] However, initiator efficiencies calculated with this value of z for the present system were very low and gave entry rate coefficients that varied only very weakly with [I], in contradiction to experimental indications to the contrary.[7,28] For this reason, the value of z for the present system was chosen as $z = 3$, along with high values for the propagation rate coefficients of very small sulfate-ended MMA oligomers in the aqueous phase; these parameters give the expected high initiator efficiency and are thus consistent with extant data on CO_2-free MMA emulsion polymerization.[7,28] Extensive data on the diffusion coefficients of oligomeric MMA species have recently been obtained[29] and were used here.

Simulated MWDs obtained with this parameter set are given in Figure 1. The single-exponential component due to transfer plus short−long termination (eq 4) is apparent, as is the nonexponential component at low M. The simulations show a variation in the high-M component with initiator concentration, suggesting that termination (between long and short chains) is a significant chain-stopping event for longer chains; in addition, the calculated sensitivity of this high-M portion to the assumed value of k_{tr} (not shown) shows that transfer to monomer is also significant.

Now, the present data comprise *cumulative* MWDs (i.e., the MWD accumulated as conversion increases). The disproportionation component will change with conversion (since the disproportionation reaction must be diffusion-controlled with the values of w_p for these systems, and diffusion coefficients depend on w_p); the transfer component is independent of conversion. Hence, cumulative MWDs will be the accumulation of single exponentials that vary with conversion and, thus, in general, will be expected to show significant nonexponential behavior even at high M. However, in the present system, the diffusion coefficient probably varies relatively slowly over much of the conversion range, and so cumulative and instantaneous distributions are similar at high M. This is supported by the appearance of the distribution labeled "cumulative" in Figure 1, which was obtained by summing the $P(M)$'s calculated at $w_p = 0.3$, 0.4, and 0.5. It is this similarity of simulated cumulative and instantaneous distributions *at high molecular weight* that enables us to use the experimental cumulative distributions at high M to make mechanistic inferences.

Results and Discussion

pH vs CO_2 Pressure. Certain aspects of free-radical polymerization kinetics depend on pH, such as the persulfate dissociation rate coefficient[30,31] or the entry and exit rate coefficients in systems with electrosteric stabilizer.[32] The pH of water will obviously change as the amount of dissolved CO_2 changes. The relation between the partial pressure of CO_2, p_{CO_2} and its concentration in water can be approximated by Henry's law:

$$[CO_2] = K_H\, p_{CO_2} \tag{6}$$

where K_H is the Henry's law constant. This dissolution involves the following equilibria:

$$CO_2 + H_2O \rightleftarrows H_2CO_3 \qquad K = \frac{[H_2CO_3]}{[CO_2]} \tag{7}$$

$$H_2CO_3 \rightleftarrows H^+ + HCO_3^- \qquad K_1 = \frac{[H^+][HCO_3^-]}{[H_2CO_3]} \tag{8}$$

i.e.,

$$[H^+][HCO_3^-] = KK_1[CO_2] \equiv K_{a1}[CO_2] \tag{9}$$

whence the relation between pH and CO_2 concentration can be written

$$\mathrm{pH} = -{}^1/_2(\log K_H + \log K_{a1}) - {}^1/_2 \log p_{CO_2} = {}^1/_2(\mathrm{p}K_H + \mathrm{p}K_{a1} - \log p_{CO_2}) \tag{10}$$

The calculated pH as a function of pressure for two temperatures is shown in Figure 2; the values of K_H and pK_{a1} were taken from the literature[33,34] and extrapolated to higher temperatures where needed. The predictions of this simple model are in acceptable accord with experimental values obtained in this laboratory.[35] The model predicts that pH decreases from 7 to 3 for pressures up to 70 bar, and further increasing the CO_2 pressure by a factor of 5 decreases pH by only ca. 10%.

The predicted and experimental dependences of pH on CO_2 pressure enable us to make certain inferences about pH effects in the present system. First, persulfate decomposition is virtually unaffected by pH over the range 3−7,[30,31] suggesting that aqueous-phase radical flux will not be affected by pH changes. Even with constant radical flux in the aqueous phase, pH changes can affect the particle surface and can thus change the

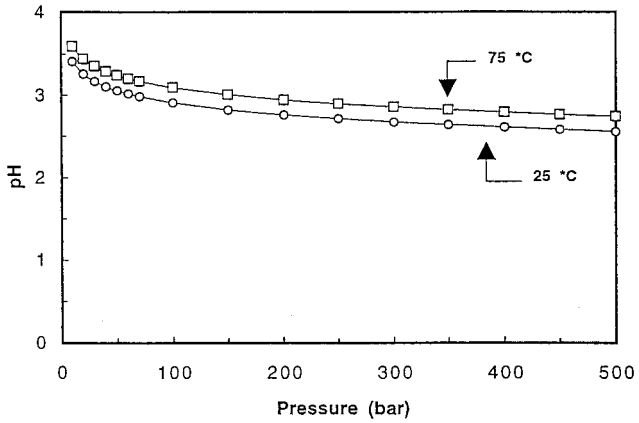

Figure 2. Calculated pH as a function of CO_2 pressure at 25 and 75 °C.

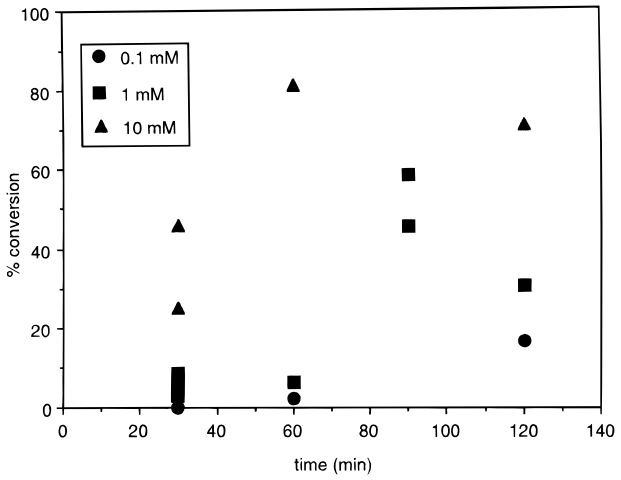

Figure 3. Conversion as a function of time for the MMA hybrid CO_2/water system initiated by 0.1, 1, and 10 mM potassium persulfate, at a pressure of ca. 140 bar CO_2.

rate coefficients for entry of radicals into, and exit of radicals from, the particles, since these are controlled by aqueous-phase or surface events.[27,36] The present system uses in situ stabilizer, and the mechanism for *entry* with latexes stabilized by what is effectively an ionic stabilizer suggests that this will be unaffected by pH changes,[27,36] a conclusion that is verified by experiment.[32] The accepted mechanism for *exit* for ionically-stabilized latexes transfer followed by diffusion away from the particle, with radical passage through the particle−water interface not being rate-determining; this mechanism is supported by extensive experimental data.[7] This thus suggests that any effect of pH on this interface will not change the rate coefficient for exit, a conclusion again supported by experiment for anionically-stabilized systems.[32] It is therefore reasonable to assume that there will be no effect of pH change on the kinetics of the present system. However, it is noted that *electrosterically* stabilized systems (e.g., with acrylic acid as co-monomer) show entry and exit rate coefficients which are strongly affected by changes in pH over the range used here,[32] and thus one would expect such effects in a CO_2−water hybrid system in the presence of water-soluble monomers.

Rate Data. Conversion-time data are reproduced in Figures 3 and 4. The significant scatter in the points can be attributed to two sources. The most obvious source of error is in the gravimetric determination of conversion, but even the most conservative estimates would predict only a small error from this source. A more significant source of scatter is variability in the induction time, that is, the time taken for any residual oxygen or inhibitor in the reaction mixture to be consumed. As is well-known, a high variability in induction time in a system such as the present, wherein there is extensive deoxygenation, is to be expected: while the amount of residual oxygen is very small, this amount is not easily reproducible (indeed, it is also well-known that the best way to obtain a reproducible induction period is to add an excess of inhibitor). Because of this variability, conversion has been used in place of time as an independent variable in many of the analyses and figures presented in the following sections. Since duplicate experiments were made with identical reaction times rather than conversions, they do not appear as duplicates after the variable substitution. However, with the exception of behavior at very low conversion, there is consistency from run to run of quantities such as particle number with conversion (see Figures 5 and 6), which is sufficient evidence for the reproducibility of experiments in this system.

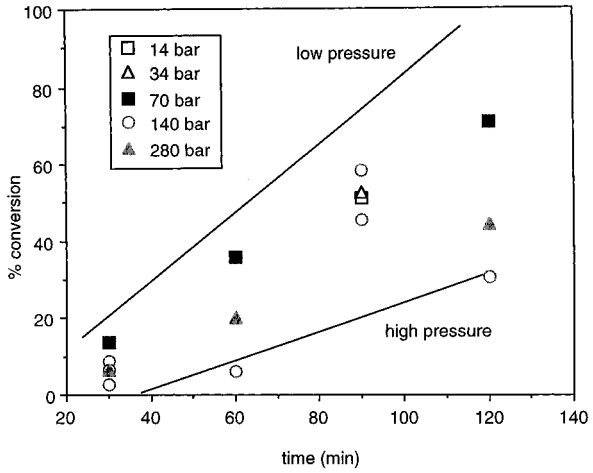

Figure 4. Conversion as a function of time for the MMA hybrid CO_2/water system initiated by 1 mM potassium persulfate, at various pressures of CO_2. The lines are drawn to suggest trends at low and high pressures.

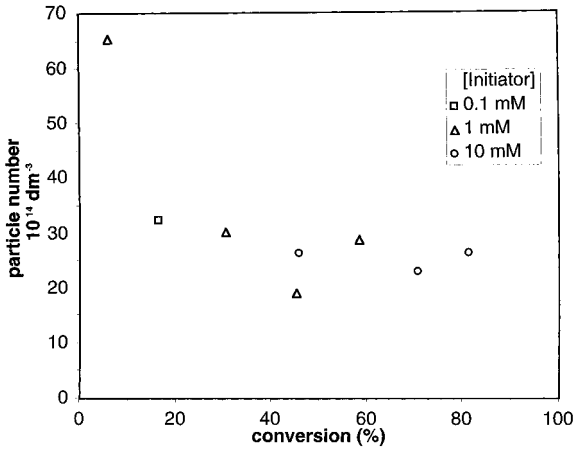

Figure 5. Dependence of particle number on conversion for the MMA hybrid CO_2/water system initiated by 0.1, 1, and 10 mM potassium persulfate, at a pressure of ca. 140 bar CO_2.

Despite the high uncertainty, these data appear to lend credibility to the hypothesis that the gel effect is reduced when reaction is carried out with significant amounts of CO_2. However, while no clear autoacceleration is seen, considering the sparse and scattered nature of the data, it would be imprudent to make any assertion of its absence. There is also a general, but

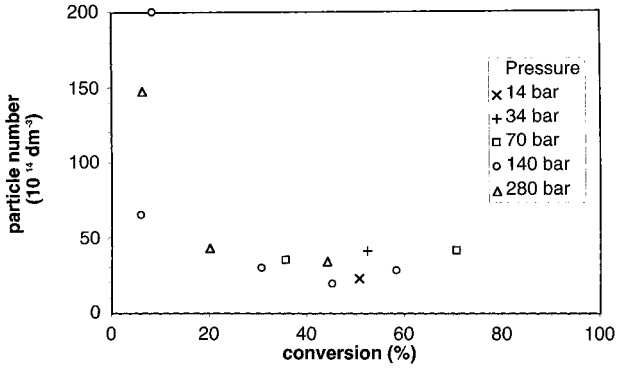

Figure 6. Dependence of particle number on conversion for the MMA hybrid CO_2/water system initiated by 1 mM potassium persulfate, at various pressures of CO_2 as indicated. High values of particle number at low conversion are probably artifacts.

not systematic, tendency to lower rate at high pressures; the slower rate could thus be explained by a lower radical population caused by decreased viscosity within particles at higher pressures. The experimental activation volume for styrene k_p suggests that this quantity would be expected to increase by only about 10% over this range of pressures.[37] This expected insensitivity of k_p to CO_2 pressure is confirmed by recent PLP measurement.[38] Note that the partitioning of CO_2 in the present hybrid system is also unknown at present. While the best evidence for a reduction in the gel effect could be obtained from accurate rate data, because of the technical difficulty in obtaining such data, our main evidence is that obtained from molecular weight distributions.

Particle Size Data. Figure 7 shows typical scanning electron micrographs (SEMs) of polymer particles from the surfactant-free polymerization conducted in the absence of CO_2 and in the presence of CO_2 (113 bar). It is apparent that the latex particles are spherical and free from agglomeration. Micrographs obtained in systems without CO_2 appear to show a small but significant population of smaller particles; the presence of such a population may not be apparent in the CHDF data.

Figure 8 shows the PSDs obtained using CHDF for pressures of ca. 70, 140, and 280 bar. The apparent shoulders seen in some of these curves are probably artifactual, since they are sensitive to the method chosen for deconvoluting the CHDF signal to obtain a PSD. From these data, the particle number concentrations N_c can be obtained from the usual formula:[7]

$$N_c = \frac{m_p}{\frac{4}{3}\pi r_u^3 d_p} \tag{11}$$

where r_u is the unswollen particle radius, d_p is the density of polymer, and m_p is the (final) mass of polymer per unit volume of the aqueous phase. Results are shown in Figures 5 and 6. The high values of N_c at low conversions are probably artifacts: measurement of particle size in for such small, relatively polydisperse, samples is subject to moderately high uncertainty (as shown by the high scatter in N_c value), and since $N_c \propto$ (diameter)$^{-3}$, this leads to a correspondingly larger uncertainty in particle number.

The first point of comparison is with particle numbers obtained in corresponding surfactant-free systems without CO_2 (note that the comparison is to be made in terms of N_c rather than particle size, since while particle

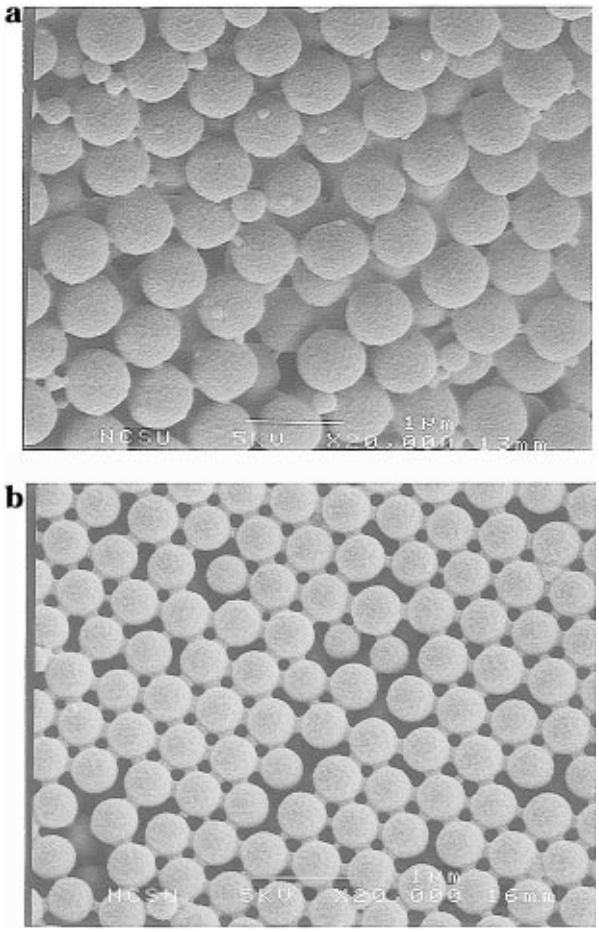

Figure 7. Scanning electron micrographs for particles formed (a) without CO_2 and (b) with CO_2 at 113 bar. Both samples are taken at ca. 80% conversion.

number is determined uniquely by the mechanism of particle formation for a given temperature, initiator concentration, etc.,[7] eq 11 shows that particle *size* also depends trivially on the amount of monomer in the recipe). There are two sets of literature data for N_c at ca. 75 °C for surfactant-free MMA emulsion polymerization,[39,40] which are in acceptable agreement: the results reported by these workers can be processed to give $N_c \approx (5-10) \times 10^{16}$ dm^{-3}. This particle number is also in accord with the present CO_2 system, as seen in Figures 5 and 6.

Our PSDs show a behavior qualitatively similar to a conventional aqueous emulsion polymerization. In the early stages of the reaction, the PSD has a distinct right skew. The tail at large particle radius is postulated to be the result of coagulation of the more numerous smaller particles.[41] As more radicals with sulfate end groups enter the particles, electrostatic stabilization improves and coagulation ceases. Thus, at higher conversions we see a more symmetrical, monodisperse PSD, consistent with colloidally-stable growth of existing particles. What is unusual is the large size of the large-radius tail, and the extent of conversion to which it persists (>10%). It is possible that this behavior results from artifacts of the CHDF analysis procedure. The breadth of the low conversion PSD's is such that slightly different methods of deconvolution of nominally duplicate distribution leads to variability in this feature. Therefore, it is quite conceivable that the tail observed at low conversion is exaggerated by the instrument broadening and that the relatively small tail expected

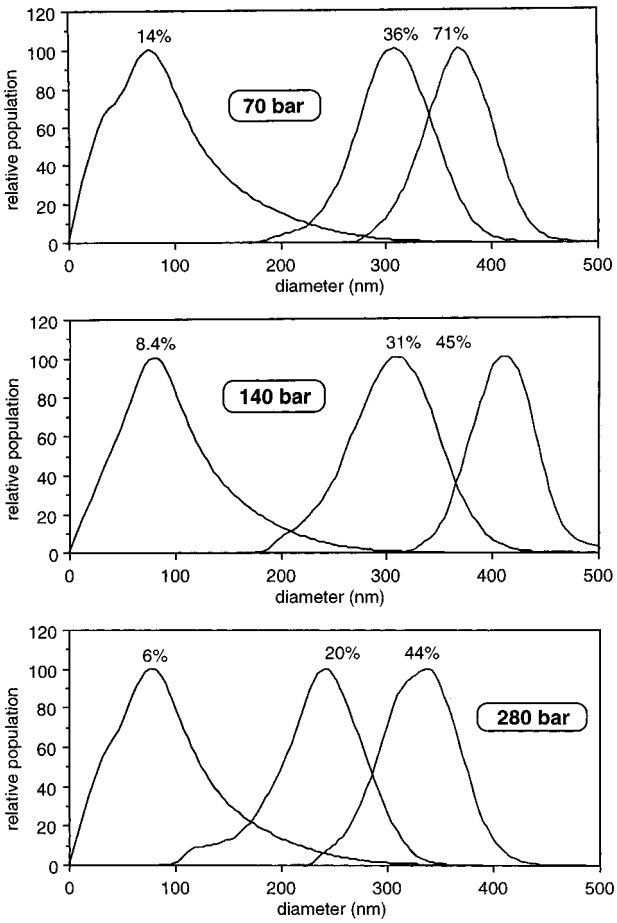

Figure 8. Particle size distributions obtained by CHDF for ca. 70, 140, and 280 bar CO_2 pressures and various conversions for the MMA hybrid CO_2/water system initiated by 1 mM potassium persulfate.

at higher conversion is not resolved by the deconvolution algorithm.

An interesting result that emerges from the data on N_c is that there is no systematic trend in N_c with CO_2 pressure or with initiator concentration; the latter observation has also been reported in surfactant-free MMA systems without CO_2.[39]

Because particle number is determined by aqueous-phase and particle growth events in very small particles,[7] the lack of dependence of N_c upon CO_2 pressure can be interpreted as insensitivity of these events to the presence of CO_2. This would not be surprising, since, for example, the change in pH is negligible, although there could be a significant effect from changes in the water-phase solubility of a given monomer, $[M_W]$, which could affect both entry and the values of j_{crit} and z. In very small particles, growth in an MMA system is dominated by entry (determined by z) and by transfer to monomer,[7,22] and transfer is not expected to be significantly affected by high CO_2 pressure. The lack of pressure dependence could arise either from a lack of pressure variation of $[M_W]$ or a fortuitous cancelation between the combined effects of a change in $[M_W]$ and/or k_p in the aqueous phase, together with changes in z and j_{crit} (both of which probably correlate with $[M_W]$[7,27]).

The lack of dependence of N_c on initiator concentration shown in Figure 5 is at first unexpected, although it has also been reported for an MMA surfactant-free system in the absence of CO_2 by Tanrisever *et al.*[39] Intuitively, one might expect that if more radicals were being produced in the aqueous phase, then more radicals would grow to length j_{crit} and form new particles. However, the same lack of dependence of N_c on initiator concentration [I] was also reported by Goodwin *et al.* for styrene surfactant-free emulsion polymerizations[42] *provided* no attempt was made to adjust the ionic strength to allow for changes in ionic strength induced by changing initiator concentration (see eq 9 of Goodwin *et al.*[42]). However, Goodwin *et al.* showed that if the ionic strength is kept constant (by varying the concentration of an added indifferent electrolyte as initiator concentration is changed), then N_c increases with [I] as expected. The most reasonable explanation for this observation is[7] in terms of a higher rate of coagulation of precursor particles caused by the increasing ionic strength as [I] is increased; this tends to reduce N_c, and approximately counterbalances the tendency of higher radical flux (increasing [I]) to increase N_c.

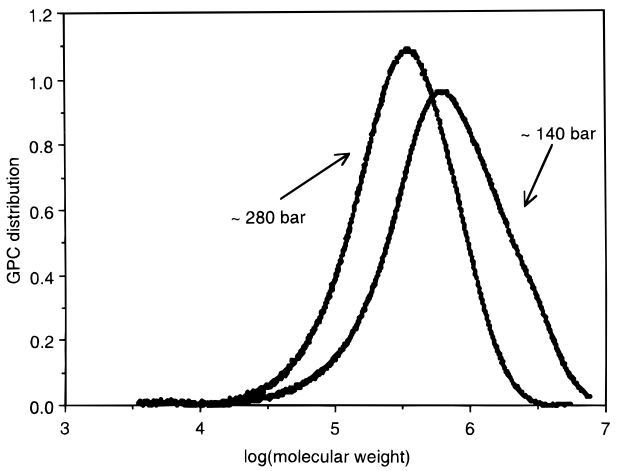

Figure 9. GPC distributions (i.e., $\mathbb{N} M^2\bar{P}(M)$, which are GPC traces with baseline subtracted and deconvoluted to remove effects of a nonlinear calibration curve) for two samples from hybrid water/CO_2 emulsion polymerization of MMA at indicated CO_2 pressures, conversion $\approx$ 45%.

Molecular Weight Distributions. Some typical GPC distributions are given in Figure 9. A selection of the molecular weight data obtained are reproduced, in the ln $\bar{P}(M)$ form (i.e., the logarithm of the cumulative number molecular weight distribution), in Figures 10–12 (note that in these figures, the regions of large scatter at high molecular weights, e.g., $M >$ ca. 1×10^6 for 10 mM initiator and 280 bar, arise where there are very large uncertainties arising from baseline subtraction, and such regions are not reproducible). The data here have been arranged so that only one of the three variables, conversion, initiator concentration, and CO_2 pressure, varies within each series. It can be seen that each of the ln $\bar{P}(M)$ plots exhibits a qualitatively similar behavior, with an upward curvature at low molecular weight and, in most cases, a more linear region at high molecular weight. The dependences of the experimental distributions on the various reaction parameters are best considered separately, since the effects displayed by each are approximately independent.

Theory[19] suggests that the instantaneous number MWD in an MMA emulsion polymerization at weight-fractions (w_p) of polymer typical of those in the present system should comprise the sum of two components: one (as shown by eq 4) a single exponential due to the combined effects of chain-stoppage by transfer to monomer and by termination between long and short chains, and the other a more complicated form due to termination between shorter chains; this latter is only signifi-

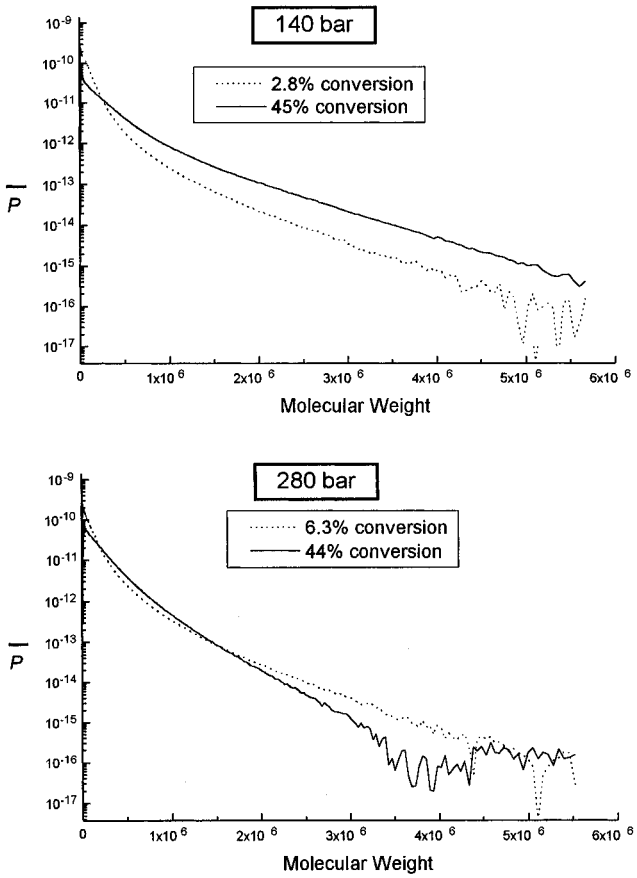

Figure 10. Experimental cumulative MWD as $\bar{P}(M)$ (on a $\log_{10}$ scale) for two different conversions at ca. 140 and 280 bar CO_2, 1 mM persulfate. In this and subsequent figures, the regions of large scatter at high molecular weights (e.g., $M >$ ca. 1×10^6 for 10 mM initiator, 280 bar) arise where there are very large uncertainties arising from baseline subtraction, and such regions are not reproducible.

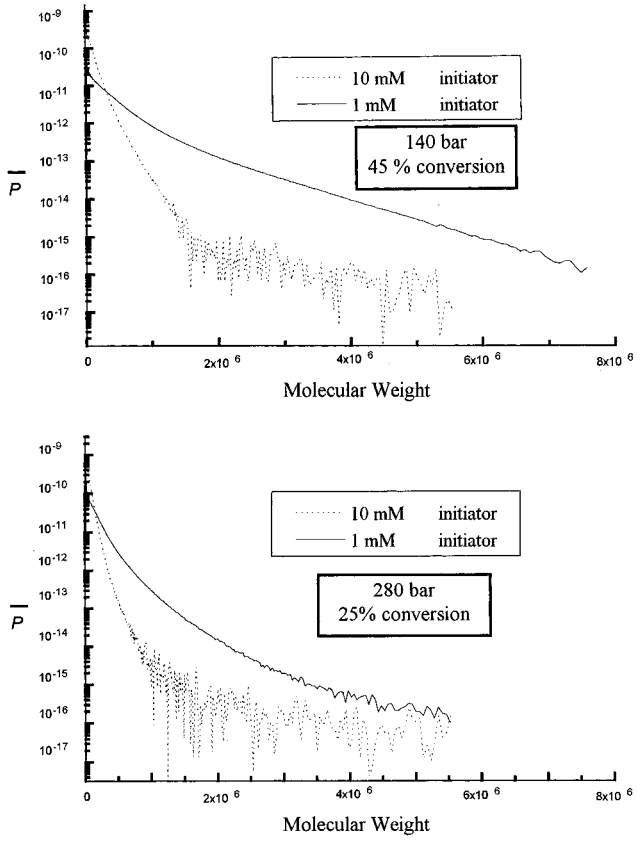

Figure 11. Experimental cumulative MWD as $\bar{P}(M)$ (on a $\log_{10}$ scale) for two different conversions at ca. 140 and 280 bar CO_2, 1 and 10 mM persulfate.

cant at quite low molecular weights. Disproportionation is probably the dominant termination mode in MMA;[43] note, however, that since termination is diffusion-controlled in emulsion polymerizations and therefore most termination is between a mobile short chain and an entangled long one, both combination and disproportionation will give a linear ln $\bar{P}(M)$ at high conversion.[7,23]

Another cause of nonexponential P(M) in a cumulative MWD from an emulsion polymerization is from the component from polymer formed during particle formation (interval 1), which can be quite different from that formed during intervals 2 and 3.[44] While the transfer portion will not change in interval 1, termination events can be quite different in very small precursor particles, and so the low-M portion can show quite a different curvature from that formed after the cessation of particle formation.

Conversion Dependence of MWD. The data presented in Figure 10 show the conversion dependence of the cumulative MWD. The linear portions of the ln $\bar{P}(M)$ are attributed to chain stoppage by transfer, and the nonlinear components at lower M, to disproportionation and the chain-stopping events in interval 1. The linearity of the ln $\bar{P}(M)$ plots improves with conversion, consistent with the suggestion that a significant component of the nonlinearity is from polymer formed in interval 1. The *full* experimental MWD cannot be adequately compared with the simulations because of the component from particle formation, whose complexities even in conventional emulsion polymerization are such that there has been no report of a successful modeling of the MWD. However, the high-M component can be compared with theory, since the contribution from interval 1 is less important; this comparison will be performed below.

Initiator Concentration Dependence of MWD. The most obvious feature of the distributions produced with higher initiator concentration in Figure 11 is the greater slope, corresponding to more rapid chain-stopping events. This is as expected, since the termination rate increases with radical concentration (eq 4) and hence with initiator concentration, and indeed is also seen in the simulated distributions of Figure 1. This effect of initiator concentration is seen at both intermediate and high pressures.

The experimental values of the high-M slope of ln $P(M)$, i.e., Λ (eq 5), provide the best means of comparison between experiment and theoretical expectations; although less than ideal, one can meaningfully compare cumulative and instantaneous values of Λ, since the data suggest that this quantity is relatively insensitive to conversion. The experimental data of Figure 11 yield $\Lambda = 1.3 \times 10^{-4}$ and 6.5×10^{-4} for 1 and 10 mM initiator. The corresponding values calculated from the model and parameters given above are $\Lambda = 1.1 \times 10^{-4}$ and 2.3×10^{-4}, using the simulations of Figure 1. While the agreement is certainly imperfect, the trends are reproduced, and the semiquantitative agreement is in fact pleasing, since the parameter values were taken (with the exception of z) entirely from the literature without any attempt at adjustment. In this context, it should be noted that the experimental values for Λ are subject to some uncertainty: for example, the expectation is that the greatest variation that Λ can show with [I] is

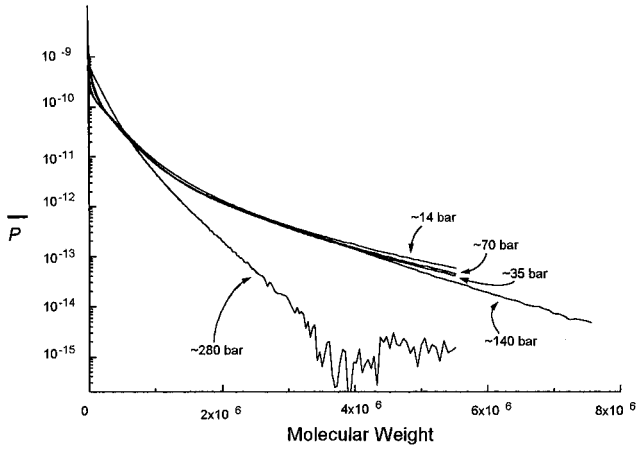

Figure 12. Experimental cumulative MWD as $\bar{P}(M)$ (on a $\log_{10}$ scale) for 40−45% conversion, 1 mM persulfate, for CO_2 pressures as indicated.

$\Lambda \propto [I]^{1/2}$; this implies that the ratio of the Λ values for 1 and 10 mM persulfate should be no more than $10^{1/2} \approx 3$, whereas the apparent experimental ratio of the above data is 5.

CO_2-Pressure Dependence of MWD. In Figure 12, we see a remarkable behavior in the pressure variation of the MWD. For low to intermediate pressures of CO_2, the distribution is essentially invariant. However, at the highest measured pressure (~280 bar), there is a marked decrease in average molecular weight, and much steeper ln $\bar{P}(M)$. The MWD formed at high pressure is significantly steeper than its low-pressure counterpart and deviates somewhat from a single exponential, even at higher molecular weights. Again, this can be attributed to a changing contribution from disproportionation. It is likely that the fundamental origin of the pressure dependence arises because, for enthalpic reasons, the swelling of polymer by CO_2 probably becomes significantly more favorable at higher pressures. The decrease in the slope of ln $\bar{P}(M)$ at the highest pressure is proposed to be the result of a consequently higher concentration of CO_2 within the particles, which significantly reduces the internal viscosity of the polymer-rich particles.

Consider the implications if the decrease is due to an increase in the termination rate. Some quantification of the reduction in viscosity in the high-pressure system can be made by taking the high molecular weight slope of the ln $\bar{P}(M)$ plot and using eq 4 as follows. If one assumes that initiator efficiency is 100% (which enables one to calculate the radical concentration [R]), and given that pseudobulk kinetics applies for MMA, then manipulation of eq 4 gives (see ref 7 for the appropriate equations):

$$\Lambda = \frac{k_{tr}}{k_p} + \frac{1}{k_p[M]}\left(\frac{k_d[I]\langle k_t\rangle}{N_c V_s}\right)^{1/2} \qquad (12)$$

where V_s is the swollen volume of a latex particle. Using the values of Λ from the lower and highest-pressure $\bar{P}(M)$ data in Figure 12, one finds that the highest pressure data show an approximate 3-fold increase in Λ: Λ(low pressure) $\approx 1.1 \times 10^{-4}$, Λ(highest pressure) $\approx 2.9 \times 10^{-4}$. Since $k_{tr}/k_p \approx 0.5 \times 10^{-4}$ for this system, this suggests that, if there is no change in k_p, the contribution to Λ from termination increases by a factor of ca. 5, i.e., that $\langle k_t\rangle$ increases by a factor of ca. 25. Since the model for the MWD discussed above implies that

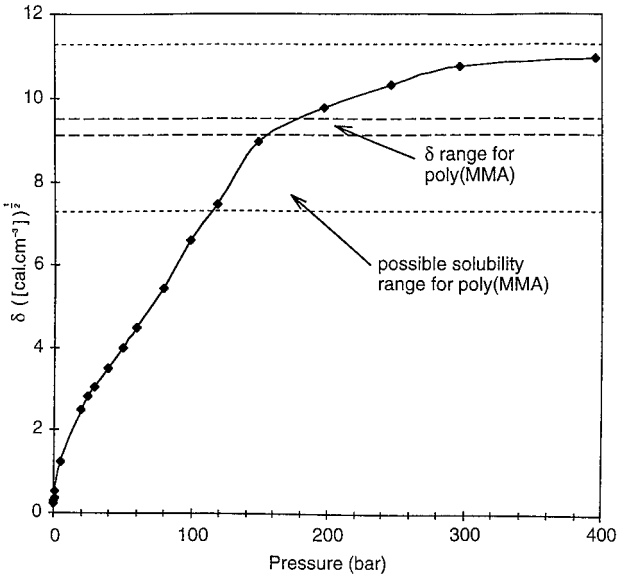

Figure 13. Calculated variability of the Hildebrand solubility parameter δ with pressure of pure CO_2 at 75 °C, calculated from tabulated data on enthalpy of vaporization and specific volume.

$\langle k_t\rangle$ is approximately (but not exactly!) proportional to the diffusion coefficients of small species, this implies that, if there is no change in k_p, these diffusion coefficients increase by about a factor of 25 at the highest pressure of CO_2 used in this system. Further quantification of this must await measurement of CO_2 partitioning in this system, so that contributions from changes in [M] can be taken into account.

Some explanation of the sudden change between 140 and 280 bar can be found by considering the Hildebrand solubility parameter (δ) data in Figure 13. These values have been calculated from tabulated literature values[45] of the specific enthalpy of vaporization (ΔH_{vap}) and specific volume (V_{sp}) of CO_2 as functions of pressure (p) and temperature, using the expression:[46]

$$\delta = \left(\frac{\Delta H_{vap} - pV_{sp}}{V_{sp}}\right)^{1/2} \qquad (13)$$

It can be seen that in the critical region, the solubility parameter rises into the region where partial, or even total, solubility of poly(MMA) in pure CO_2 would be expected. Total solubility of the polymer was not observed, probably because the system is not a binary mixture but contains various quantities of water and monomer. However, it is clear how quickly the favorability of the CO_2−poly(MMA) interaction can change. Also, the abrupt change of slope seen in Figure 13 at just over 140 bar indicates the possibility of a partial phase change in the CO_2, which may also explain the sudden change in behavior.

Conclusions

The surfactant-free emulsion polymerization of methyl methacrylate in a hybrid carbon dioxide/aqueous medium with a water-soluble initiator shows some interesting similarities and differences to corresponding systems in the absence of CO_2. Colloidally-stable latexes are produced, with particle sizes (or more precisely particle number concentrations) generally similar to those seen in the absence of CO_2. However, the addition of supercritical CO_2 to a conventional surfactant-free emulsion polymerization has a definite

effect upon both the reaction kinetics and the product formed. In particular, the sudden and profound change in the molecular weight distribution at 280 bar is due to a fundamental change in chain-stopping mechanism (that the addition of supercritical CO_2 at such pressures greatly reduces the viscosity inside the polymer particles, increasing the rate of bimolecular termination). Further quantification of the data in these systems will also require proper measurements of the effects of CO_2 on the concentration of monomer in the aqueous and particle phases.

Acknowledgment. We are grateful for the financial support of the National Science Foundation (J.M.D., Presidential Faculty Fellow, 1993−1997) as well as from the Consortium on the Synthesis and Processing in Polymeric Materials in Carbon Dioxide, which is sponsored by the Environmental Protection Agency, DuPont, Hoechst-Celanese, Air Products and Chemicals, B. F. Goodrich, Eastman Chemical, Bayer, Xerox, and General Electric. The support of the Australian Research Council is also gratefully acknowledged. We would like to thank Dale Batchelor at North Carolina State University and Wallace W. Ambrose of the UNC-Chapel Hill DRC Microscopy Laboratory for assistance with the SEMs and Ms. Jelica Hutovic in Sydney University for CHDFs.

References and Notes

(1) Shaffer, K. A.; DeSimone, J. *Trends Polym. Sci.* **1995**, *3*, 146.
(2) Canelas, D. A.; Betts, D. E.; Desimone, J. M. *Macromolecules* **1995**, *28*, 2818.
(3) DeSimone, J. M.; Guan, Z.; Elsbernd, C. S. *Science* **1992**, *257*, 945.
(4) Romack, T. J.; Maury, E. E.; DeSimone, J. M. *Macromolecules* **1995**, *28*, 912.
(5) Horvath, I. T.; Rabai, J. *Science* **1994**, *266*, 72.
(6) Condo, P. D.; Paul, D. R. *Macromolecules* **1994**, *27*, 365.
(7) Gilbert, R. G. *Emulsion Polymerization: A Mechanistic Approach*; Academic: London, 1995.
(8) DeSimone, J. M.; Romack, T. J. Multi-phase Polymerization Process. 1. U. S. Patent 5,514,759 5,514,759, 1996.
(9) DeSimone, J. M.; Romack, T. J. Multi-phase Polymerization Process. 2. U. S. Patent 5,527,865 5,527,865, 1996.
(10) DeSimone, J. M.; Romack, T. J. Multi-phase Polymerization Process. 3. U. S. Patent 5,530,077 5,530,077, 1996.
(11) Romack, T. J.; Kipp, B. E.; DeSimone, J. M. *Macromolecules* **1995**, *28*, 8432.
(12) Fitch, R. M.; Tsai, C. H. In *Polymer Colloids*; Fitch, R. M., Ed.; Plenum: New York, 1971; pp 73.
(13) Ugelstad, J.; Hansen, F. K. *Rubber Chem. Technol.* **1976**, *49*, 536.
(14) Feeney, P. J.; Napper, D. H.; Gilbert, R. G. *Macromolecules* **1987**, *20*, 2922.
(15) Hsaio, Y. L.; Maury, E. E.; DeSimone, J. M.; Mawson, S.; Johnston, K. P. *Macromolecules* **1995**, *28*, 8159.
(16) Lermert, R. M.; DeSimone, J. M. *Supercrit. Fluids* **1990**, *4*, 186.
(17) Dos Ramos, J. G.; Silebi, C. A. *Polym. Int.* **1993**, *30*, 445.
(18) Miller, C. M.; Sudol, E. D.; Silebi, C. A.; El-Aasser, M. S. *J. Colloid Interface Sci.* **1995**, *172*, 49.
(19) Clay, P. A.; Gilbert, R. G. *Macromolecules* **1995**, *28*, 552.
(20) Shortt, D. W. *J. Liquid Chromat.* **1993**, *16*, 3371.
(21) Russell, G. T.; Gilbert, R. G.; Napper, D. H. *Macromolecules* **1992**, *25*, 2459.
(22) Ballard, M. J.; Napper, D. H.; Gilbert, R. G. *J. Polym. Sci., Polym. Chem. Ed.* **1984**, *22*, 3225.
(23) Clay, P. A.; Gilbert, R. G.; Russell, G. T. *Macromolecules* **1997**, *30*, 1935.
(24) Whang, B. C. Y.; Ballard, M. J.; Napper, D. H.; Gilbert, R. G. *Aust. J. Chem.* **1991**, *44*, 1133.
(25) Beuermann, S.; Buback, M.; Gilbert, R. G.; Hutchinson, R. A.; Klumpermann, B.; Olaj, F. O.; Russell, G. T.; Schweer, J. *Macromol. Chem. Phys.* **1997**, *198*, 1545.
(26) Gilbert, R. G. *Pure Appl. Chem.* **1996**, *68*, 1491.
(27) Maxwell, I. A.; Morrison, B. R.; Napper, D. H.; Gilbert, R. G. *Macromolecules* **1991**, *24*, 1629.
(28) Russell, G. T.; Gilbert, R. G.; Napper, D. H. *Macromolecules* **1993**, *26*, 3538.
(29) Griffiths, M. C.; Gilbert, R. G. To be published.
(30) Santos, A. M.; Vindevoghel, P.; Graillat, C.; Guyot, A.; Guillot, J. *J. Polym. Sci., Part A: Polym. Chem.* **1996**, *34*, 1271.
(31) Kolthoff, I. M.; Miller, I. K. *J. Am. Chem. Soc.* **1951**, *73*, 3055.
(32) Coen, E.; Lyons, R. A.; Gilbert, R. G. *Macromolecules* **1996**, *29*, 5128.
(33) Fogg, P. G. T.; Gerrard, W. *Solubility of gases in liquids*; John Wiley and Sons: New York, 1991.
(34) Butler, J. N. *Carbon dioxide equilibria and their applications*; Addison-Wesley: New York, 1982.
(35) DeSimone, J.; et al. In press.
(36) Casey, B. S.; Morrison, B. R.; Gilbert, R. G. *Prog. Polym. Sci.* **1993**, *18*, 1041.
(37) Buback, M.; Kuchta, F.-D. *Macromol. Chem. Phys.* **1995**, *196*, 1887.
(38) Quadir, M.; DeSimone, J.; van Herk, A.; German, A. L. Manuscript in preparation.
(39) Tanrisever, T.; Okay, O.; Sonmezoglu, I. C. *J. Appl. Polym. Sci.* **1996**, *61*, 485.
(40) Sütterlin, N. In *Polymer Colloids II*; Fitch, R. M., Ed.; Plenum: New York, 1980.
(41) Lichti, G.; Gilbert, R. G.; Napper, D. H. *J. Polym. Sci., Polym. Chem. Ed.* **1983**, *21*, 269.
(42) Goodwin, J. W.; Hearn, J.; Ho, C. C.; Ottewill, R. H. *Colloid Polym. Sci.* **1974**, *252*, 464.
(43) Zammit, M. D.; Davis, T. P.; Haddleton, D. M.; Suddaby, K. G. *Macromolecules* **1997**, *30*, 1915.
(44) Miller, C. M.; Clay, P. A.; Gilbert, R. G.; El-Aasser, M. A. *J. Polym. Sci., Polym. Chem. Ed.* **1997**, *35*, 989.
(45) Perry, R. H.; Chilton, C. H.; Kirkpatrick, S. D. In *Chemical Engineer's Handbook*, 4th ed.; Perry, R. H., Chilton, C. H., Kirkpatrick, S. D., Eds.; McGraw-Hill: New York, 1963.
(46) Bovey, F. A.; Winslow, F. H. In *Macromolecules: An Introduction to Polymer Science*; Bovey, F. A., Winslow, F. H., Ed.; Academic: New York, 1979.

MA970259A